# BROADBAND WIRELESS SENSING OF RADIOACTIVE CHEMICALS UTILIZING INHERENT RF TRANSMISSIONS FROM PULSE DISCHARGES

Christine K. Eun[1], Ranjit Gharpurey[2], and Yogesh B. Gianchandani[1]
[1]*Department of Electrical Engineering and Computer Science, University of Michigan - Ann Arbor, USA*
[2]*Department of Electrical and Computer Engineering, University of Texas - Austin, USA*
*email: eunc@eecs.umich.edu, ranjitg@mail.utexas.edu, yogesh@umich.edu*

***Abstract*—This paper reports a wireless sensing scheme that exploits gas discharges in microstructures and discharge-based sensors such as micromachined Geiger counters. Experiments are conducted on devices that have a glass-Si-glass stack of 8x8 mm$^2$ footprint, with discharge gaps in the range of 300-550 $\mu$m. Electrical discharges triggered by exceeding the breakdown voltage and by ionization due to beta particles provide an RF spectrum spanning a bandwidth greater than 1.2 GHz, which extends into the ultra-wideband (UWB) range of communication. These are broadband signals that can be detected by AM and FM radios at distances greater than 50 cm from the sensor. Measurements of electric field strength and audio recordings from radio receivers are reported.**

## I. INTRODUCTION

Discharge-based transducers have been reported for a wide variety of applications such as chemical sensing and nuclear radiation detection. The vast majority of hazardous radioisotopes emit beta particles during their decay process. Geiger counters use current discharges and are the preferred instruments for detecting beta radiation [1]. They are reliable, temperature insensitive, require only simple circuitry, and measure over a wide range of radiation species and energies. A micromachined version of a Geiger counter has been reported in the past that not only detects the presence of radioactive species, but is also capable of discerning isotope identity to some extent by performing energy spectroscopy [2,3].

Other discharge-based radiation sensors have been developed and reported in the past [4-6]. Current discharges have been employed in vapor and liquid phase chemical sensors in which the optical spectrum of the emission indicates the presence of certain species [7]. Discharge-based actuators have been used as surge protectors as well as high voltage and high current switches [8].

Historically, intentional firing of current discharges to wirelessly transmit information was first employed by Guglielmo Marconi. Building on the foundation of work developed by Maxwell and Hertz, Marconi utilized electromagnetic emissions produced by spark gaps in his design of the first radio transmitter [9]. Spark gaps essentially consist of two separated, conducting electrodes surrounded by some background gas (usually air). When a suitable voltage (breakdown voltage) is applied between these electrodes, a spark develops, initiating electron avalanche and forming a path for current flow through the gas. During the discharge, an electromagnetic signal is generated and transmitted over a very large bandwidth. Efforts to use discharges within waveguides in order to generate microwaves date back to Bose in 1901, and more recent activity has also been reported [10]. However, the exploration of RF radiation from micromachined structures provides many avenues for continued research, particularly in combination with sensing. In this effort, we examine wireless transmissions caused by discharges in devices that have a glass-Si-glass stack of 8x8 mm$^2$ footprint, with discharge gaps in the range 300-550 $\mu$m. These discharges are triggered by applying the breakdown voltage and by ionization due to beta particles. An intrinsic wireless transmission capability provides an efficient and low-power mechanism for remote detection and/or monitoring dangerous radioactive materials.

## II. DEVICE CONCEPT

A simple analysis is first used to determine the theoretical feasibility of the concept in terms of the device geometry, discharge gap, drive circuitry, and the presence of parasitics.

### *1) Modeling emission spectra*

An analytical estimate has been reported for the high frequency (UHF > 500MHz) electromagnetic radiation emitted during discharges [11]. If $l$ is the characteristic length scale in the current channel, $r$ is the distance from the observer to the channel, and $\lambda$ the radiation wavelength, then the dipole ordering is $l < \lambda < r$. Given a square-wave shaped current pulse that is described by:

$$I(t) = I_0, \quad 0 < t < \tau_0 \qquad (1)$$

The magnetic flux density due to dipole radiation is approximately given by:

$$B = \frac{-2l\sin\theta}{c^2 r}\frac{\partial I(t-r/c)}{\partial t} \quad \text{(Gauss)} \qquad (2)$$

where $c$ is the speed of light and $\theta$ is the viewing or observation angle. The Fourier components of $B$ are given by:

$$b = \frac{4iI_0\sin\theta\exp(i\omega[r/c+\tau_0/2-(l/c)\cos\theta])}{cr\omega\cos\theta} \times \sin(\frac{\omega l}{c}\cos\theta)\sin(\frac{\omega\tau_0}{2}) \qquad (3)$$

where $\omega$ is the angular frequency. According to this, current discharges with a characteristic channel length on the order of 1 mm are expected to have spectra extending well over 3 GHz. The primary cause of the wide-spanning frequency emission is thought to be the abrupt changes in current (i.e. at discharge initiation and termination) occurring in the electrode gap. By tailoring the shape of the current waveform, the emission spectrum can be controlled. For example, in order to make the system compatible with the ultra-wideband [12] communication specifications, the current pulse can be optimized to have a steeper or higher current derivative. This will result in higher frequency components and consequently larger bandwidths. Also, minimizing the parasitic capacitances inherent within the micromachined structure and test circuit will reduce the RC time constant resulting in a wider frequency response.

### 2) *Basic microGeiger electrode configuration*

The basic microGeiger (Fig. 1) has a square chamber with a central cathode and a peripheral anode. The region proximal to the cathode has a weak field and is called the drift region, whereas that adjacent to the anode is the high-field avalanche amplification region. Beta particles pass through the glass window into the drift region, ionizing the background gas. (In contrast with conventional Geiger counters, this gas is at atmospheric pressure.) The electrons are slowly accelerated into the amplification region. In the amplification region the electrons are quickly accelerated through a higher field region resulting in an electron cascade, which is the micro-discharge. Designing the drift region to be much larger than the amplification region permits pulses to be relatively independent of the entry position of the beta particle.

### 3) *Modeling parasitics within current discharge*

Models describing gas breakdown characteristics have been developed in the past [13-15]. Also, simulation models describing current discharges in the time domain have been developed for applications such as $\mu$EDM (micro-electro-discharge machining) [16]. One possible arc model consists of a thyristor or SCR (silicon controlled rectifier) in series with a Zener diode. The thyristor provides the threshold turn on and turn off behavior, the Zener diode provides the voltage drop of a sustained discharge, and the inductor and resistor tailor the temporal behavior of the current pulse.

Figure 2 shows the discharge circuit including the DC bias circuitry, the microGeiger gap modeled with the SCR and Zener diode combination, and the estimated parasitics inherent to the microGeiger structure as well as the large capacitive loading from the measurement equipment. Table 1 summarizes the values of these parasitics including approximately 22 pF loading from the oscilloscope and probe connected to the cathode end of the microGeiger. $C_{Gap}$ is the approximate capacitance calculated for the $p^{++}$ Si anode-cathode configuration alone where as $C_{P,substrate}$ and $C_{P,drift}$ are parasitic capacitances associated with the substrate and electrode fringe fields. $R_{P,anode}$ and $R_{P,cathode}$ are the parasitic resistances through the lead contacts. $L_p$ and $R_p$ are used to model the temporal behavior of the discharge current.

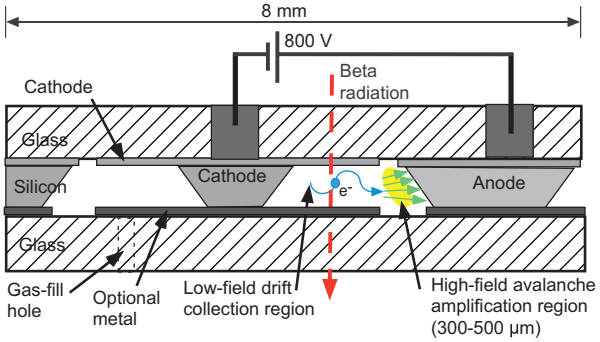


Figure 1. The micromachined Geiger counter has a central cathode and a concentric anode. Beta radiation passing through the weak-field drift region near the cathode ionizes the Ne; electrons travel to the high-field amplification region near the anode where they are accelerated, creating a current pulse.

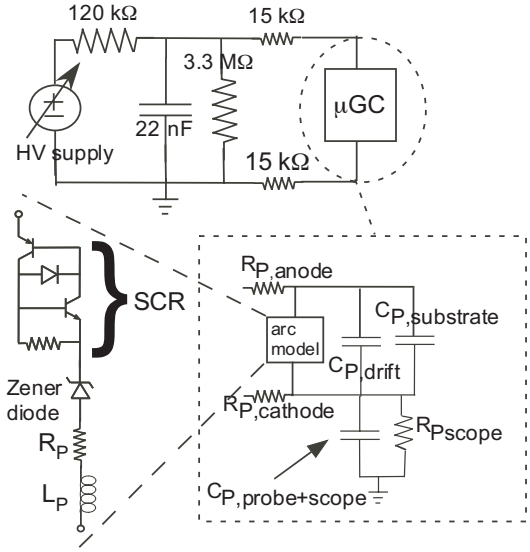


Figure 2: Schematic of microGeiger test circuit including DC bias circuitry as well as equivalent circuit of parasitics involved in the microGeiger discharge gap. Large capacitive loading from measurement equipment slows current pulse response.

Table 1: Modeling of parasitics in microGeiger circuit.

| Parameter name | Capacitance value (estimated) |
|---|---|
| $C_{Gap}$ | 12. fF |
| $R_{P,\ anode}$ | 8.2 kΩ |
| $R_{P,\ cathode}$ | 409.4 kΩ |
| $C_{P,\ substrate}$ | ~ 0.5 – 5 pF |
| $C_{P,\ drift}$ | ~ 10 – 30 fF |
| $C_{P,\ probe+scope}$ | 22 pF |
| $R_{P,\ scope}$ | 1 MΩ |
| $L_p$ | ~1 $\mu$H |
| $R_p$ | ~30 Ω |

## III. Experimental Results

Figure 3 shows the test set-up used in this effort. Tests were conducted in a Ne gas-filled environment, which reflects the packaging environment that will be typically used for the device. A power supply provided a DC bias between the electrodes of the device, which was placed at specified distances from various sources with strengths ranging from 0.1-1 $\mu$C. The resulting RF transmissions were monitored by both an RF field strength analyzer and radio receiver. Figure 4 shows oscilloscope traces illustrating the typical impulse-like shape produced by the microGeiger due to passing beta particles. The recorded duration of each pulse discharge is on the order of tens of milliseconds. It is believed that due to capacitive loading from the test measurement equipment, the actual pulse duration of the discharge is significantly slowed down.

The frequency spectrum (Fig. 5) shows the bandwidth of transmissions from a sample at a fixed distance (2.5 cm) ranging from 485 MHz to above 1.65 GHz. This clearly demonstrates that communication using a pulse-based broadband transmission and reception scheme for a system such as UWB will be clearly possible. The FCC has specified emission limits for the UWB system from 100 MHz to 10.6 GHz [12]. The field strength measurements were taken from a cavity of 8x8 mm$^2$ footprint at a fixed distance with a battery operated, handheld device (Protek, Inc. 3290). The field strength analyzer was supplied with an 8-inch whip antenna designed for the 800 MHz cellular band. The relative increase in signal strength at higher frequencies may be attributed to the associated antenna factor. The signal was sampled at 125 channels/sec at 1 MHz/channel while in Narrow Band FM demodulation mode.

Figure 6 shows audio recordings from AM and FM radio receivers detecting current discharges at a fixed distance from the sensor. These measurements were obtained from discharges that were triggered by beta particles coming from a $^{204}$Tl source. However, discharges triggered by simply raising the bias above the breakdown voltage have the same characteristics. Plots of signal intensity versus time that were obtained from sound recordings show distinct, narrow spikes directly representative of the audible discharges heard through the AM/FM receiver. Audible signal detection was achieved while sweeping over the entire available AM (525 kHz to 1705 kHz) and FM (88 MHz to 108 MHz) bandwidths. This demonstrates how the microGeiger enables the use of commonly available electronics for wireless signal detection.

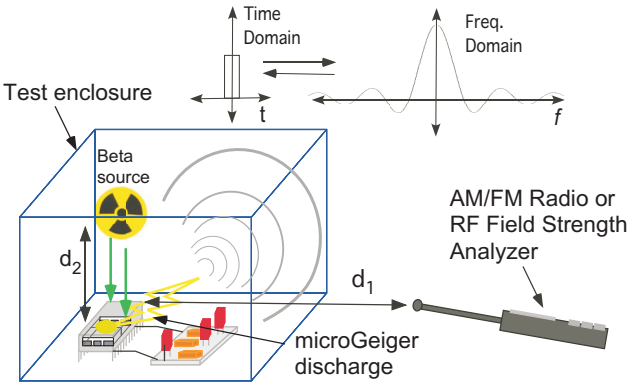


Figure 3: Test setup showing the microGeiger connected to DC bias circuit. The presence of the beta source initiates the current discharge and consequent RF emission. The electromagnetic signal is picked up by either an AM/FM radio receiver or an RF field strength analyzer.

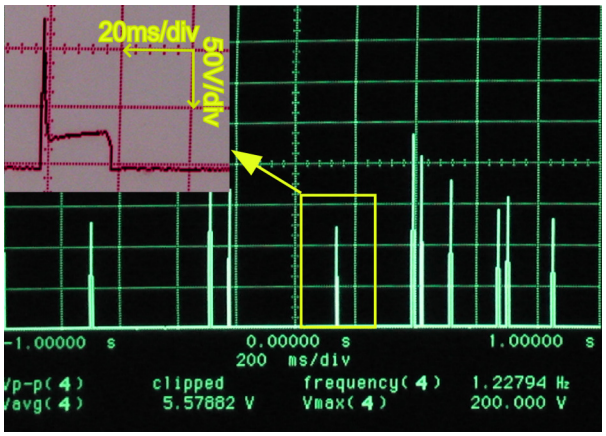


Figure 4: Oscilloscopes traces showing shapes of typical current pulses, as measured by the voltage across a test resistor attached to the cathode. Although the time scale shown are in milli-seconds, the actual current pulse duration is thought to be in the nano- to micro-seconds range. The measurement equipment provides a high capacitive loading.

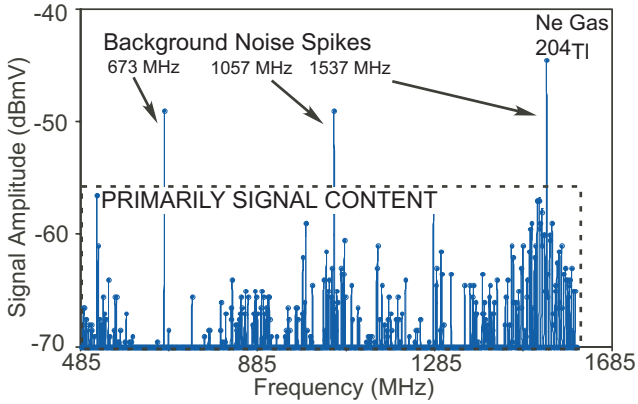


Figure 5: Field strength measurements at 2.5 cm distance showing relative signal amplitude spanning a bandwidth of at least 1200 MHz. Background radiation has been subtracted. The relative increase in signal strength at higher frequencies is due to the antenna factor.

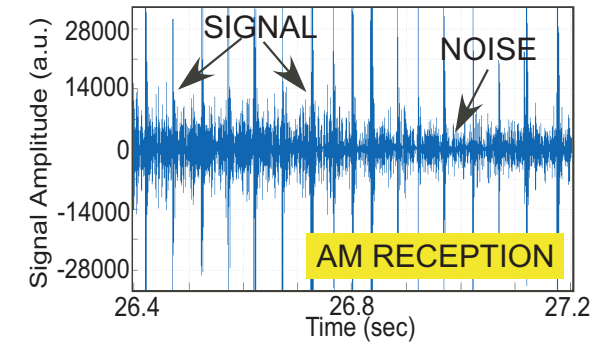


(a)

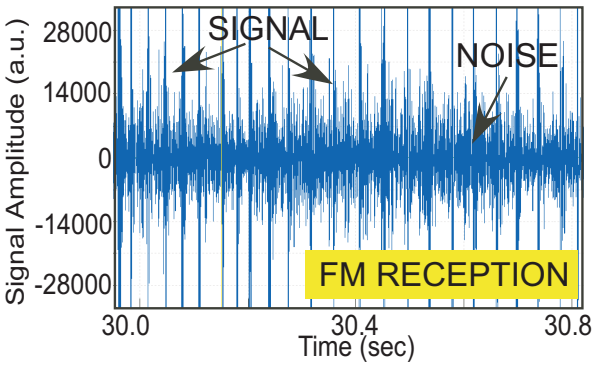


(b)

Figure 6: Audio recordings as received by an AM/FM radio. (a) AM recordings; (b) FM recordings at 109 MHz. The radiation source was $^{204}$Tl, located 1 cm from the microGeiger; the tip of the radio antenna was 7.6 cm away from the sensor. The length of the antenna when fully extended was 56 cm. The audio spectra were visualized using the software program, SIGVIEW© which plots signal intensity versus real time.

## IV. Conclusions

There are several emerging applications for which distributed wireless sensor networks can be very beneficial. These range from applications like seismic monitoring; monitoring environments that are inaccessible because of remoteness or due to man-made or natural disasters; monitoring high-traffic public places like sports stadiums or railway stations; to military applications such as battlefield surveillance. To the extent that sensors for some of these applications may use discharge-based detection, e.g. Geiger counters, or may be integrated with micromachined discharge generators, the inherent RF transmissions will provide an alternative to conventional wireless communication schemes which employ special, often power hungry, transmitter hardware. This effort has shown that the electromagnetic signal emitted from the microGeiger discharge gap spans a bandwidth greater than 1.2 GHz, which extends into the ultra-wideband (UWB) window (from 100 MHz to 10.6 GHz). An 8x8 mm$^2$ microGeiger is able to sense radiation and wirelessly transmit broadband signals that can be detected by AM and FM radios at distances greater than 50 cm from the sensor. Both measurements of field strength and audio recordings from radio receivers were reported. Discharges caused by applying a breakdown voltage across these electrodes (in the absence of radiation) exhibit the same characteristics. These initial measurements hold significant promise for wireless microsensor networks. Opportunities exist both for networks that use inexpensive off-the-shelf radio components, as well as more customized circuits that exploit the characteristics of discharge-based emissions.

## V. Acknowledgments

This work was supported primarily by the Engineering Research Centers Program of the National Science Foundation under Award Number EEC-9986866. The facilities used for this research include the Michigan Nanofabrication Facility (MNF) at the University of Michigan. The authors also thank Prof. David Wehe for access to the Nuclear Engineering test facilities.

## References

[1] G.F. Knoll, Radiation Detection & Measurement, J. Wiley, 2000.

[2] C.G. Wilson, Y.B. Gianchandani, "MicroGeiger: A Microfabricated Gas-Based Beta Particle Detector," *Solid-State Sensors & Actuators Workshop,* Hilton Head Island, South Carolina, June '04, pp. 53-56.

[3] C.G. Wilson, C. K. Eun, Y. B. Gianchandani, "D-MicroGeiger: A microfabricated beta-particle detector with dual cavities for energy spectroscopy," *IEEE Intl. Conf. MEMS,* January 2005

[4] M. Wada, J. Suzuki, and Y. Ozaki, "Cadmium telluride ß-ray detector," *IEEE Transducers*, 1987 A478, pp. 258-261.

[5] J.A. Kemmer, "Silicon detectors for nuclear radiation," *IEEE Transducers, 1987* A478, pp. 252-257.

[6] G. Charpak, J. Derre, Y. Giomataris, P. Rebourgeard, "Micromegas, a multipurpose gaseous detector," *Nuclear Instruments & Methods in Physics Research, Section A*, v 478, n 1-2, 1 Feb. 2002, p 26-36.

[7] B. Mitra and Y.B. Gianchandani , "The micromachined flashFET: a low-power, three-terminal device for high speed detection of vapors at atmospheric pressure,"*IEEE International Conference on Micro Electro Mechanical Systems*, 2005, p 794-7.

[8] S. Bonisch and W. Kalkner, "Measurement and simulation of the behavior of a short spark gap used as ESD protection device," *IEEE Intl. Symp. on Electromagnetic Compatibility*, V1, 2003, p 37-42.

[9] J.E. Brittain, "Electrical engineering Hall of Fame: Guglielmo Marconi," *Proceedings of the IEEE*, V92, No.9, Aug 2004, pp1501-4.

[10] A.G. Heaton and J.H. Reeves, "Microwave radiation from discharges," *3rd International Conference on Gas Discharges*, Sept. 1974, pp73-77.

[11] A. Kadish and W.B. Maier, II, "Electromagnetic radiation from abrupt current changes in electrical discharges," *Journal of Applied Physics*. 70(11), Dec. 1991, pp. 6700-6711.

[12] FCC 02-48, First Report and Order, "Revision of Part 15 of the Commission's Rules Regarding Ultra-Wideband Transmission Systems," Feb 14, 2002:
http://hraunfoss.fcc.gov/edocs_public/attachment/FCC-02048A1.pdf

[13] T. Ono, Y. Dong, M. Esashi, "Microdischarge and electric breakdown in a micro-gap," *Jounral of Micromechanics and Microengineering,* 10(3) 9/00, pp. 445-451.

[14] W. Janischewskyj, A. M. Hussein, N.H.C. Santiago, "Performance and analysis of a micro-gap discharge circuit," *IEEE Transactions on Power Delivery,* V3, No. 2, April 1988, pp. 694-706.

[15] J.M. Meek and J.D. Craggs, *Electrical Breakdown of Gases* Oxford: Clarendon Press, 1953.

[16] K. Takahata and Y.B. Gianchandani, "Batch Mode Micro-Electro-Discharge Machining," *JMEMS*, 11(2), April 2002, pp. 102-110.